Electronics and Information Technologies, 2026, 35, 219–230
http://publications.lnu.edu.ua/collections/index.php/electronics/index

UDC: 535.37; 537.311

SPECTRAL AND ELECTRICAL CHARACTERISTICS OF Mn- AND Mn-Zr-DOPED $BaGa_2O_4$ PHOSPHORS

Dmytro Slobodzyan**, Markiyan Kushlyk, Vyacheslav Vasyltsiv, Ivanna Medvid, Andriy Luchechko
Department of Sensor and Semiconductor Electronics,
Ivan Franko National University of Lviv
107 Gen. Tarnavskoho Street, Lviv, 79017, UKRAINE

Slobodzyan, D., Kushlyk, M., Vasyltsiv, V., Medvid, I., Luchechko, A. (2026). Spectral and Electrical Characteristics of Mn- and Mn-Zr-Doped $BaGa_2O_4$ Phosphors. *Electronics and Information Technologies*, 35, 219–230. https://doi.org/10.30970/eli.35.16

ABSTRACT

Background. $BaGa_2O_4$ is a wide-band-gap oxide with promising luminescent and electronic properties, making it a potential host for phosphor and optoelectronic materials. Controlled doping provides an effective approach for modifying its luminescence, defect structure, and charge-transport properties.

Materials and Methods. Undoped $BaGa_2O_4$ (BGO), BGO: 0.1 mol% Mn, and BGO: 0.1 mol% Mn, 0.2 mol% Zr were synthesized by the high-temperature solid-phase method. Photoluminescence and photoluminescence excitation spectra were measured at room temperature. DC conductivity was investigated in vacuum in the temperature range of 370–490 K, while AC conductivity was measured in the frequency range of 100 Hz–50 kHz using an excitation electrical field amplitude of 5.0 V.

Results and Discussion. Undoped BGO exhibits intense broadband blue luminescence with a maximum near 410 nm, attributed to host emission centers. Mn doping shifts the emission maximum to 430-440 nm, significantly decreases the intensity, and introduces an additional excitation band at 270–340 nm, indicating the existence of an effective excitation channel associated with Mn centers. Co-doping with Zr further decreases the intensity but does not substantially change the emission spectral composition. According to the CIE 1931 analysis, the color purity decreases from 80% for BGO to 75% and 71% for Mn- and Mn-Zr-doped samples, respectively. Electrical measurements show that Mn doping increases DC conductivity by more than an order of magnitude, whereas Mn-Zr co-doping reduces the conductivity while maintaining values above those of undoped BGO. The DC activation energies remain close, ranging from 1.15 to 1.19 eV. AC conductivity exhibits frequency dispersion described by the universal Jonscher law, with the temperature dependence of the exponent *s* indicating changes in localized charge-transport mechanisms.

Conclusion. Mn and Mn-Zr doping effectively modify the optical and electrical properties of barium gallate through changes in localized states and defect structure. The ability to tune luminescence and charge transport highlights the potential of doped $BaGa_2O_4$ for phosphor and optoelectronic applications.

Keywords: $BaGa_2O_4$, Mn-Zr dopants, luminescence, electrical conductivity, localized states, phosphors

© 2026 Dmytro Slobodzyan et al. Published by the Ivan Franko National University of Lviv on behalf of Електроніка та інформаційні технології / Electronics and Information Technologies. This is an Open Access article distributed under the terms of the Creative Commons Attribution 4.0 License which permits unrestricted reuse, distribution, and reproduction in any medium, provided the original work is properly cited.

INTRODUCTION

$BaGa_2O_4$ is a wide-band-gap oxide with a hexagonal structure formed by a framework of GaO_4 tetrahedra and containing channels occupied by Ba^{2+} ions [1]. Owing to its high thermal and chemical stability, structural robustness, and ability to accommodate optically active impurities, $BaGa_2O_4$ is considered a promising host matrix for luminescent and multifunctional oxide materials [2]. Modification of its optical and electronic properties through controlled doping makes this material attractive not only for phosphor applications but also for emerging optoelectronic technologies, where the combination of light emission, charge transport, and defect-state engineering is particularly important.

The optical and electrical properties of wide-band-gap oxides are strongly governed by their defect structure, including intrinsic point defects, impurity centers, charge-compensating defects, and localized electronic states [3]. These states can influence carrier generation, trapping, transport, and radiative recombination, establishing a direct relationship between the luminescent and electrical characteristics of the material. Doping with transition-metal ions, such as Mn, provides an effective approach for introducing additional localized states and modifying the concentration and distribution of defect centers, thereby enabling control over both the emission characteristics and charge-transport processes [4]. Such defect engineering is particularly relevant for optoelectronic materials, since the performance of luminescent and light-sensing devices strongly depends on the balance among carrier localization, charge transport, and radiative recombination.

Co-doping with ions of different valence states and ionic radii provides an additional means of tailoring the defect structure and local charge compensation in the $BaGa_2O_4$ lattice. In particular, the simultaneous incorporation of Mn and Zr may modify the concentration and spatial distribution of localized states and intrinsic point defects, thereby affecting the pathways of charge transfer and the magnitude of electrical conductivity. Changes in these processes can, in turn, influence the interaction between charge carriers and luminescent centers. Similar relationships between doping-induced defect modification, charge transport, and optical response have been observed in other wide-band-gap gallium-containing oxides [5].

From the viewpoint of optoelectronic applications, simultaneous consideration of luminescence and electrical properties is especially important. A material intended for light-emitting, photodetection, scintillation, or other optoelectronic functions should possess not only suitable emission characteristics but also controlled charge-carrier transport and trapping behavior. Therefore, investigation of both DC and AC conductivity can provide complementary information about the defect states and localized charge-transfer mechanisms responsible for the functional properties of doped $BaGa_2O_4$. In particular, the activation energy obtained from the temperature dependence of DC conductivity provides information about the energy barrier governing the dominant transport process, whereas the frequency dependence of AC conductivity can reveal the contribution of localized carriers and their interaction with the surrounding defect environment.

Although the structural and luminescent properties of $BaGa_2O_4$ and its doped derivatives have been investigated [1, 2, 6], the relationship between impurity incorporation, luminescence, charge transport, and localized-state dynamics remains insufficiently understood. In particular, systematic studies combining the spectral characteristics with the temperature and frequency dependences of DC and AC conductivity in Mn-doped and Mn-Zr-co-doped $BaGa_2O_4$ are limited. Analysis of these characteristics is important for understanding how doping affects the localized charge-transfer processes, and for assessing the potential of these materials as functional components in optoelectronic applications.

Therefore, the aim of this work is to investigate the spectral and electrical characteristics of Mn- and Mn-Zr-doped $BaGa_2O_4$ phosphors and to elucidate the influence of doping on their spectral response and charge-transport behavior. The combined analysis of spectral and electrical properties provides insight into the role of doping-induced defects and localized states and helps evaluate the prospects of Mn- and Mn-Zr-doped $BaGa_2O_4$ for phosphor and optoelectronic applications.

MATERIALS AND METHODS

The synthesis of the studied $BaGa_2O_4$ samples was carried out using a high-temperature solid-phase method. Powders of barium carbonate ($BaCO_3$), gallium oxide (Ga_2O_3), manganese (III) oxide (Mn_2O_3), and zirconium (IV) oxide (ZrO_2) with a purity of at least 99.99% were used as initial precursors. The calculation of impurity concentrations for doping was performed using the isomorphic substitution model for Ga^{3+} ions in the cationic sublattice [6]. The weighed oxide mixtures were ground in an agate mortar with the addition of isopropyl alcohol for 6 h. After that, the powder mixtures were formed into disk-shaped samples with a diameter of 6 mm and a thickness of ~1.5 mm under a pressure of 100 atm, and then sintered at 1523 K for 12 h. Three types of samples were prepared: undoped base matrix (BGO), samples with 0.1 mol% Mn (BGO:Mn), and samples doped with 0.1 mol% Mn and 0.2 mol% Zr (BGO: Mn, Zr). According to the results of X-ray diffraction analysis, all samples contained a single $BaGa_2O_4$ phase.

Photoluminescence (PL) and photoluminescence excitation (PLE) spectra were recorded at room temperature using a Solar CM2203 spectrofluorometer. The PL spectra were automatically corrected for the spectral response, and the PLE spectra for the Xenon lamp emission profile.

To study the electrophysical properties of the samples, a highly conductive silver paste was applied to the opposite surfaces of each disk. The diameter of the formed metal contacts was 5 mm, ensuring a uniform electric-field distribution throughout the volume of the material under study. DC conductivity measurements were performed in vacuum during cooling from approximately 490 to 370 K. The frequency dependence of AC conductivity was studied using a HIOKI IM3536 LCR meter over the range 100 Hz–50 kHz at an excitation electrical field amplitude of 5.0 V.

RESULTS AND DISCUSSION

In the luminescence spectrum of undoped BGO samples when excited at a wavelength of 250 nm, i.e., in the region of the fundamental absorption edge, an intense broad emission band with a maximum near 410 nm is observed, which covers the spectral range from approximately 325 to 625 nm (**Fig. 1a, curve 1**). The broad nature of this band indicates its non-elementary nature and the possible superposition of several closely spaced luminescence bands associated with different emission centers. The observed luminescence in the blue-violet region of the spectrum can be attributed to intrinsic defects or localized electronic states in the BGO matrix.

After the introduction of a manganese impurity, the luminescence intensity significantly decreases compared to undoped samples (**Fig. 1a, curve 2**). At the same time, the broadband maximum shifts to the long-wavelength region, approximately 430 nm. Such a change in the spectrum indicates that the introduction of Mn significantly affects the relaxation processes of the electronic excitation energy in the matrix. The decrease in the intensity of intrinsic luminescence may be associated with the interception of excitation energy by Mn centers and subsequent relaxation via the states of these impurity ions. In this case, the shift of the maximum to the long-wavelength region may indicate a decrease in the contribution of the short-wavelength component of intrinsic luminescence and a simultaneous increase in the relative contribution of the radiation associated with Mn^{2+}.

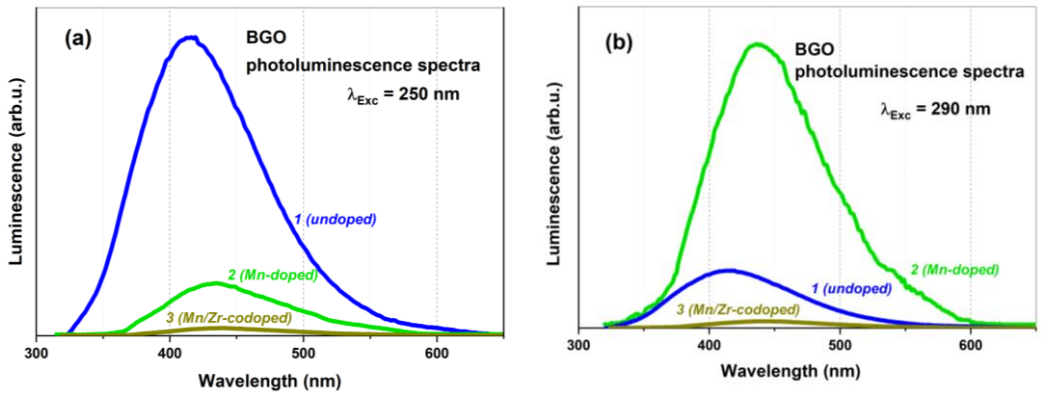


Fig. 1. Luminescence spectra of undoped (curve 1), doped with Mn impurity (curve 2), and co-doped with Mn-Zr impurities (curve 3) BGO samples when excited in the region of the fundamental absorption edge at 250 nm (a) and when excited at a wavelength of 290 nm (b)

Mn^{2+} ions in the crystal field are characterized by broad luminescence bands associated mainly with intracenter *d–d* transitions. Their spectral position and intensity depend significantly on the coordination environment of Mn^{2+}, the symmetry of the local crystal field, and the nature of the interaction between the impurity center and the matrix. Therefore, the observed long-wavelength emission in the region of 430–440 nm can be attributed to Mn^{2+} centers, although additional data are required to unambiguously determine the specific transition scheme, in particular, temperature dependence and time-resolved luminescence measurements.

Co-doping with manganese and zirconium (Mn-Zr) leads to a further decrease in the luminescence intensity (**Fig. 1a, curve 3**). This indicates that the introduction of Zr additionally changes the relaxation mechanism of electronic excitation in BGO. Most likely, this is due to changes in the concentration and nature of defect states, in the local crystal field near the Mn^{2+} centers, or to the appearance of additional non-radiative relaxation channels [7].

When excited at a wavelength of 290 nm, which corresponds to the region of much weaker absorption of the BGO matrix, the spectral pattern changes significantly (**Fig. 1b**). For undoped samples, the luminescence intensity under such excitation decreases sharply, which indicates a low efficiency of excitation of the intrinsic emission centers outside the region of the fundamental absorption edge. In contrast, in BGO:Mn samples excited at 290 nm, a broad luminescence band with a maximum near 440 nm forms. Its intensity is several times higher, and its spectral half-width is somewhat narrower than that of undoped BGO samples. This is an important argument that, at 290 nm, excitation is more selectively directed to impurity Mn centers, whereas at 250 nm, both the matrix's own centers and the impurity centers associated with manganese ions are simultaneously excited.

Thus, changing the excitation wavelength allows for partial separation of the matrix and Mn impurity contributions to the luminescence spectrum. Excitation at 250 nm preferentially activates BGO intrinsic centers through absorption in the region of the fundamental absorption edge, while excitation at 290 nm more effectively activates Mn-related impurity centers.

The luminescence excitation spectra presented in **Fig. 2** further confirm the difference in the luminescence mechanisms in undoped and doped samples. For undoped BGO, when recording radiation at 410 nm (**Fig. 2a, curve 1**), the main excitation band is located in the region of the fundamental absorption edge of the matrix. At the same time, in the region of BGO transparency, the luminescence excitation efficiency is low. After Mn doping, the excitation spectrum changes significantly; in particular, alongside the weak components associated with matrix absorption, a broad band appears in the range of approximately

260 – 340 nm (**Fig. 2a, curve 2**). Its presence indicates the appearance of an additional absorption channel associated with impurity Mn centers. Accordingly, Mn luminescence can be effectively excited without direct excitation of the interband transitions of the matrix.

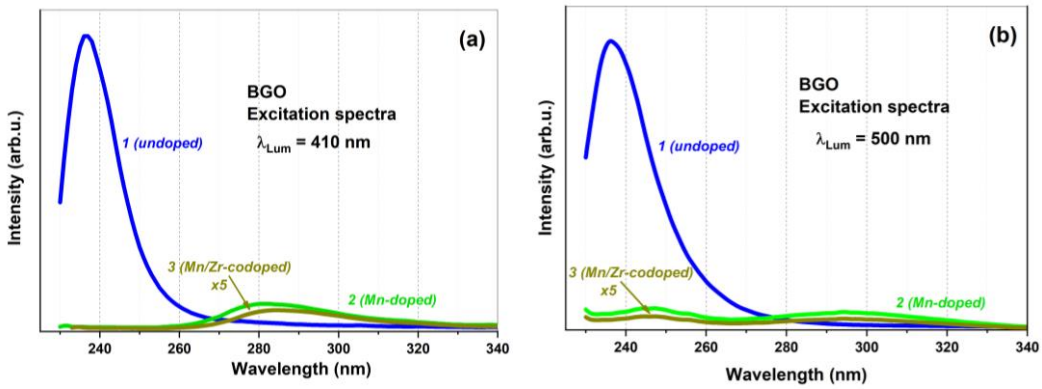


Fig. 2. Luminescence excitation spectra of undoped (curve 1), doped with Mn impurity (curve 2), and co-doped with Mn-Zr impurities (curve 3) BGO samples when recording the luminescence at 410 nm (a) and 500 nm (b)

When recording luminescence at 500 nm (**Fig. 2b**), the contribution of impurity centers is even more pronounced. At the same time, co-doping with Zr changes the excitation spectra (**Fig. 2b, curve 3**), indicating the influence of Zr on the formation and relaxation of excited states. The decrease in luminescence intensity in Mn-Zr samples may be associated with reduced radiative relaxation efficiency or increased non-radiative relaxation [7]. Thus, the results of excitation spectroscopy confirm the existence of an excitation channel of Mn centers in BGO and explain the increase in the relative contribution of long-wavelength luminescence when excited at 290 nm.

The additional UV excitation band with a maximum near 280 – 290 nm in the Mn-doped samples may be associated with a charge-transfer transition from O^{2-} ligands to Mn^{2+} ions ($O^{2-} \rightarrow Mn^{2+}$), similar to charge-transfer excitation bands reported for Mn-doped oxide materials, including zinc and magnesium gallates. Thus, the appearance of this band indicates the formation of an additional excitation pathway involving Mn^{2+} centers. Consequently, Mn-related luminescence can be efficiently excited not only through excitation of the BGO host matrix but also through direct charge-transfer excitation of the Mn^{2+} centers.

The color characteristics of the studied BGO samples were evaluated using the CIE 1931 chromaticity diagram (**Fig. 3**). Undoped BGO is characterized by chromaticity coordinates located in the blue region of the diagram, and the calculated color purity is approximately 80%. For Mn-doped samples, a moderate shift of the chromaticity coordinates towards the green region and a decrease in color purity to approximately 75% are observed. This change is consistent with the shift of the luminescence spectrum to the long-wavelength region after the introduction of Mn and an increase in the contribution of broadband radiation from Mn centers. Co-doping of Mn and Zr leads to a further change in the chromaticity coordinates and a decrease in the calculated color purity to approximately 71%. At the same time, the change in the coordinates is relatively small, indicating Zr mainly affects the luminescence intensity and the efficiency of relaxation processes, and does not radically change the spectral composition of the emission.

Thus, the CIE 1931 results show that the introduction of Mn and subsequent co-doping with Zr do not cause a fundamental change in the color of the BGO emission, but gradually shift it from the blue region towards the greenish-blue and are accompanied by a decrease

in color purity. The main effect of doping is manifested not so much in the change in the chromaticity coordinates, but in a significant change in the intensity and ratio of the intrinsic and impurity components of luminescence.

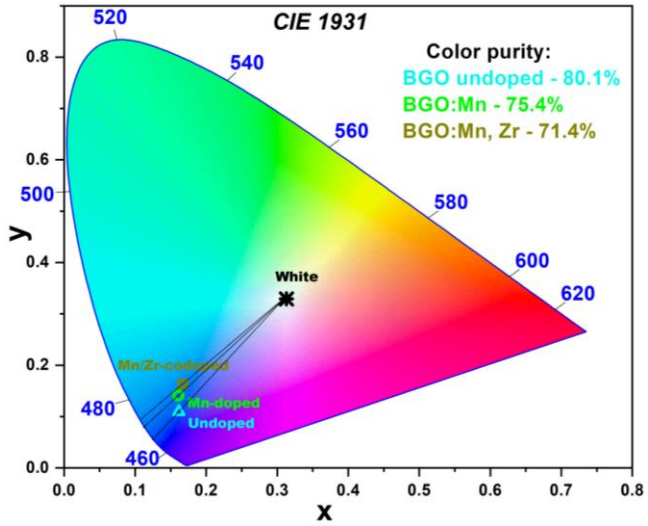


Fig. 3. CIE 1931 chromaticity diagrams of undoped, Mn-doped, and Mn-Zr-codoped BGO samples. The color-purity values are also indicated for each sample

Overall, the results indicate that Mn is an active center that significantly alters the mechanism of excitation-energy relaxation in BGO, and that the introduction of Zr further modifies these processes. In this case, excitation at 290 nm is particularly effective for selectively exciting Mn centers, as evidenced by the formation of an intense, broad luminescence band with a maximum at about 440 nm.

Fig. 4 shows the temperature dependence of the DC conductivity of the studied samples. For all samples, an increase in conductivity with temperature is observed, indicating that the dominant transport process is thermally activated, a characteristic of wide-gap oxide semiconductors and dielectrics. Undoped BGO samples demonstrate the lowest conductivity values (σ_{DC}), while doping with manganese ions leads to an increase

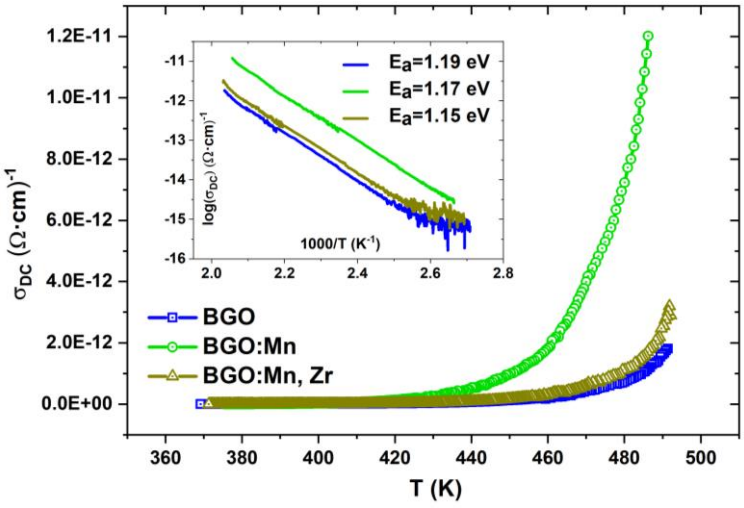


Fig. 4. Temperature dependences of the DC conductivity of BGO, BGO:Mn, and BGO:Mn, Zr samples

of more than an order of magnitude in the entire studied temperature range. For co-doped BGO:Mn, Zr samples, the conductivity values occupy an intermediate position between undoped and Mn-doped samples.

In Arrhenius coordinates, the temperature dependences are close to linear in the range of conductivity changes by about four orders of magnitude. The calculated activation energy values are 1.19 eV for BGO, 1.17 eV for BGO:Mn, and 1.15 eV for BGO:Mn, Zr. The close agreement among the activation energy values indicates that Mn doping and Mn/Zr co-doping do not significantly change the energy barrier of the dominant transport process. This is also consistent with the behavior of deep centers in related oxides [8]. Given the wide-bandgap nature of BGO and its high activation energy, the observed conductivity can be attributed to the thermally activated release of charge carriers from localized defect states. One possible type of such states is deep electronic centers formed by oxygen vacancies.

The increase in DC conductivity upon Mn doping indicates that the introduction of manganese changes the electrical properties of BGO, although the obtained activation energy values remain close to those for the undoped matrix. Unlike gallium oxide [7], manganese ions do not create additional fast recombination channels in BGO. One possible explanation for the observed increase in conductivity may be the formation of localized electronic states associated with Mn centers or a change in the equilibrium of intrinsic defects. In particular, during high-temperature solid-state synthesis, some manganese ions may transition to the reduced state, Mn^{2+}. In the case of substitution of trivalent gallium, such an ion acts as an effective negatively charged acceptor center. Its compensation may occur, in particular, due to the formation of oxygen vacancies. In this case, a change in the concentration of oxygen vacancies can affect the concentration of charge carriers and the electrical conductivity of the material [9]. A similar effect of transition metal impurities on electrical conductivity was previously observed in related wide-gap gallium-containing oxides [10].

Co-doping with zirconium reduces conductivity relative to samples doped with Mn alone. This behavior is consistent with the assumption that Zr modifies the defect equilibrium in the material and partially compensates for defects that contribute to charge transfer in Mn-containing samples [11]. The fact that the conductivity of the co-doped samples remains higher than that of the undoped matrix may indicate incomplete charge compensation or the formation of complex local defect clusters composed of manganese and zirconium ions, which can participate in charge-transfer processes, thereby reducing the overall resistance of the material [12]. Thus, the obtained data indicate a significant effect of doping on the absolute conductivity but do not allow us to unambiguously establish the charge-transfer mechanism. In addition to electronic conductivity, BGO may have quite significant ionic conductivity through channels present in the material structure.

AC conductivity studies (**Fig. 5**), conducted over the range 100 Hz to 50 kHz, reveal a significant frequency dispersion, which is typical of dielectric materials and wide-gap semiconductors with a high density of localized states. At 303 K, the conductivity of all samples increases monotonically with increasing applied electric-field frequency. The absolute values of AC conductivity at this temperature lie in the range from ~ 5×10^{-12} to ~ 5×10^{-10} $(\Omega\cdot cm)^{-1}$. The highest conductivity values are demonstrated by the Mn-doped sample, while the undoped matrix is characterized by the lowest values. With a further increase in frequency to 50 kHz, the curves partially converge, which may indicate a decrease in the contribution of long-range charge transfer and an increase in the role of localized relaxation and polarization processes [13].

When the temperature increases to 393 K, the overall AC conductivity increases, reaching values in the range of ~ 5×10^{-11} to 10^{-9} $(\Omega\cdot cm)^{-1}$. At this temperature, in the frequency region, approximately from 100 Hz to 1 kHz, there is a tendency for the curves

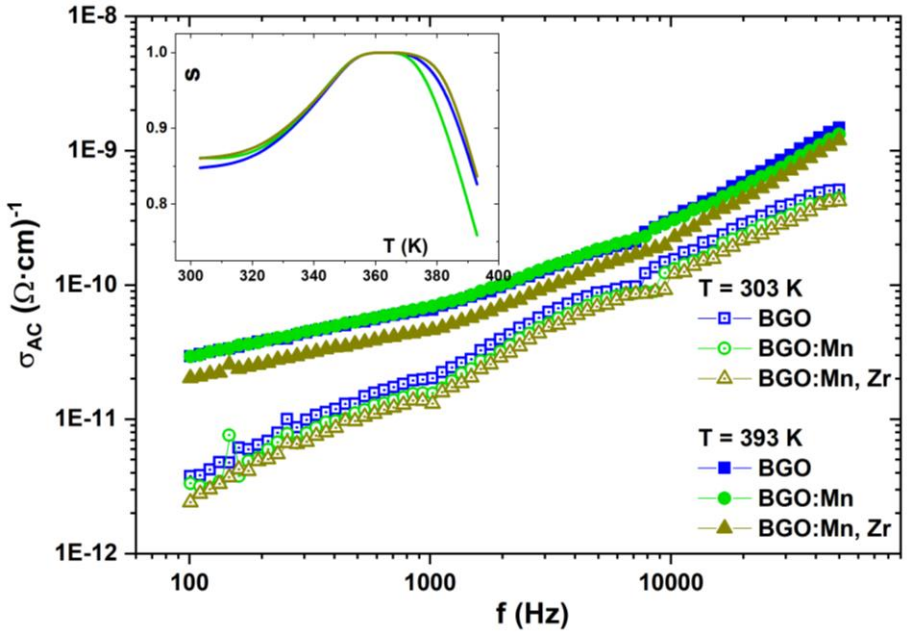


Fig. 5. Frequency dependences of AC conductivity of BGO, BGO:Mn, and BGO:Mn, Zr samples at different temperatures

to plateau. The presence of such a plateau may be associated with the dominance of the DC component of conductivity at low frequencies.

In the high-frequency region, the AC conductivity exhibits a dispersion characteristic of disordered and defective oxide systems and can be described by the universal Johnsher law [14]:

$$\sigma_{AC}(\omega) = \sigma_{DC} + A \cdot \omega^{s}, \quad (1)$$

where σ_{AC} is the total AC conductivity, σ_{DC} is the DC component of conductivity, A is the temperature-dependent coefficient, ω is the angular frequency, and s is a dimensionless frequency dependence index that characterizes the nature of the frequency dispersion and is associated with the mechanism of localized charge transfer.

The temperature dependence of the parameter s has a non-monotonic character. At 303 K, its values are approximately 0.85 – 0.86, after which they increase to values close to unity in the region of 360 – 370 K, and decrease with further increases in temperature.

The increase of the parameters to values close to unity may indicate a change in the nature of the local relaxation of charge carriers. Such behavior can be considered within the framework of models of tunneling of carriers between localized states, in particular, the non-overlapping small polaron tunneling (NSPT) model [13], as well as the nearly constant loss (NCL) model [15]. At the same time, the obtained results do not allow us to unambiguously give preference to one of these models, and therefore, both interpretations should be considered as possible.

With a further increase in temperature above ~ 370 K, a decrease in the parameter *s* is observed. Such an inversion of the temperature dependence may indicate a change in the dominant charge transfer mechanism and is characteristic of the correlated barrier hopping (CBH) model, within which the *s* index decreases with increasing temperature [13]. This may be due to thermally activated charge transfer between localized states through potential barriers. With increasing temperature, the probability of thermally activated jumps increases, which leads to a change in the frequency dependence of the conductivity [16].

For Mn-doped samples, the transition to the region of decreasing *s* is observed already at approximately 365 K, and the minimum values of the parameter reach approximately 0.75. This may indicate that the introduction of Mn changes the local environment of the charge carrier localization centers and affects the nature of their frequency-dependent transport. Substitution of Ga by Mn ions with a different ionic radius can cause local structural deformations and change the distribution of potential barriers between neighboring localization centers. Thus, even at close values of the activation energy of DC conduction, doping can significantly affect the local dynamics of charge carriers.

CONCLUSION

It was found that undoped $BaGa_2O_4$ exhibits intense broadband luminescence with a maximum near 410 nm, attributed to intrinsic emission centers in the matrix. Mn doping is accompanied by a shift of the luminescence maximum to 430 nm and a significant decrease in its intensity when excited in the region of the fundamental absorption edge at a wavelength of 250 nm. When excited at 290 nm, a broad luminescence band with a maximum near 440 nm is formed in $BaGa_2O_4$ samples. The appearance of an excitation band in the range of 270–340 nm indicates the presence of an effective excitation channel associated with Mn centers and the possibility of their more selective excitation compared to the intrinsic centers of the matrix. Co-doping of Mn-Zr leads to a further decrease in luminescence intensity, which may be due to changes in the matrix defect structure and an enhancement of non-radiative relaxation. At the same time, the introduction of Zr does not significantly change the spectral composition of the emission.

According to the CIE 1931 chromaticity diagrams, undoped $BaGa_2O_4$ exhibits blue emission with a color purity of about 80%. Mn doping and Mn/Zr co-doping cause a moderate shift of the chromaticity coordinates towards the green region and a decrease in color purity to about 75 and 71%, respectively. The results demonstrate the possibility of controlling the spectral and color characteristics of $BaGa_2O_4$ luminescence through doping and by varying the excitation wavelength, which opens prospects for its use in optoelectronic applications.

Doping BaGa2O4 with Mn impurities increases DC conductivity relative to the undoped matrix. Co-doping with Zr/Mn impurities reduces conductivity compared to samples doped only with Mn, however, its values remain higher than for the undoped matrix. The activation energies of DC conductivity for the studied samples are close, at 1.15 – 1.19 eV. This indicates that doping does not significantly change the energy barrier of the dominant transport process. The observed change in the absolute conductivity may be associated with a modification of the concentration of localized states and intrinsic point defects.

The frequency dependence of the AC conductivity is described by the universal Johnsher law. The non-monotonic temperature dependence of the parameter *s* indicates a change in the nature of localized charge transfer as temperature varies. The increase in *s* to values close to unity can be associated with tunneling or almost frequency-independent transfer mechanisms, while the further decrease in *s* with increasing temperature is compatible with the correlated barrier jump model.

ACKNOWLEDGMENTS AND FUNDING SOURCES

This work was supported by the National Research Foundation of Ukraine, Grant no. 2025.07/0450 “Wide-bandgap gallium-based oxide materials with controlled luminescent and electrical characteristics for energy-saving optoelectronics”.

COMPLIANCE WITH ETHICAL STANDARDS

The authors declare that the research was conducted in the absence of any conflict of interest.

AUTHOR CONTRIBUTIONS

Conceptualization, [D.S., A.L.]; methodology, [D.S., M.K., V.V.]; investigation, [D.S., M.K., V.V., I.M.]; writing – original draft preparation, [D.S., A.L.]; writing – review and editing, [D.S., M.K., V.V., A.L.]; visualization, [D.S., M.K., I.M., A.L.].

All authors have read and agreed to the published version of the manuscript.

REFERENCES

[1] Kahlenberg, V., Fischer, R. X., Parise, J. B. (2000). The stuffed framework structure of $BaGa_2O_4$. *J. Solid State Chem.*, *154*(2), 612–618. https://doi.org/10.1006/jssc.2000.8903

[2] Klym, H., Karbovnyk, I., Luchechko, A., Kostiv, Y., Pankratova, V., Popov, A. I. (2021). Evolution of free volumes in polycrystalline $BaGa_2O_4$ ceramics doped with Eu^{3+} ions. *Crystals*, *11*(12), 1515. https://doi.org/10.3390/cryst11121515

[3] Tuller, H. L., Bishop, S.R. (2011). Point defects in oxides: Tailoring materials through defect engineering. *Annu. Rev. Mater. Res.*, *41*, 369–398. https://doi.org/10.1146/annurev-matsci-062910-100442

[4] Smyth, D. M. (2000). Effects of dopants on the properties of metal oxides. *Solid State Ion.*, *129*(1-4), 5–12. https://doi.org/10.1016/S0167-2738(99)00312-4

[5] Wang Y., Su J., Lin Z., Zhang J., Chang J., Hao Y. (2022). Recent progress on the effects of impurities and defects on the properties of Ga_2O_3. *J. Mater. Chem. C*, 10(37), 13395-13436. https://doi.org/10.1039/d2tc01128j

[6] Wang, S., Wang, T., Yu, X., Li, Z., Guo, L., Chen, J., Zhao, F., Feng, W., Xu, X., Qiu, J. (2021). Tailored Luminescence Output of Bi^{3+}-Doped $BaGa_2O_4$ Phosphors with the Assistance of the Introduction of Sr^{2+} Ions as Secondary Cations. *Inorg. Chem.*, *60*(18), 14467–14474. https://doi.org/10.1021/acs.inorgchem.1c02271

[7] Luchechko, A., Vasyltsiv, V., Kushlyk, M., Syvorotka, I., Kostyk, L.; Slobodzyan, D., Zhydachevskyy, Y. (2025). Luminescence and thermally stimulated conductivity of polycrystalline β-Ga_2O_3: Mn and β-Ga_2O_3: Mn, Si. *J. Vac. Sci. Technol. A*, *43*, 042802. https://doi.org/10.1116/6.0004570

[8] Chikoidze, E., Sartel, C., Madaci, I., Mohamed, H., Vilar, C., Ballesteros, B., Belarre, F., del Corro, E., Vales-Castro, P., Sauthier, G., Li, L., Jennings, M., Sallet, V., Dumont, Y., Pérez-Tomás, A. (2020). P-Type Ultrawide-Band-Gap Spinel $ZnGa_2O_4$: New Perspectives for Energy Electronics. *Cryst. Growth Des. 20*(4), 2535–2546. https://doi.org/10.1021/acs.cgd.9b01669

[9] Linderälv, C., Lindman, A., Erhart, P. (2018). A Unifying Perspective on Oxygen Vacancies in Wide Band Gap Oxides. *J. Phys. Chem. Lett.*, *9*(1), 222–228. https://doi.org/10.1021/acs.jpclett.7b03028

[10] Shawuti, S., Can, M. M., Gülgün, M. A., Firat, T. (2014) Grain size dependent comparison of ZnO and $ZnGa_2O_4$ semiconductors by impedance spectrometry. *Electrochim. Acta*, *145*, 132–138. https://doi.org/10.1016/j.electacta.2014.08.084

[11] Luchechko, A., Vasyltsiv, V., Kushlyk, M., Kostyk, L., Slobodzyan, D. (2024). Electrical conductivity, luminescence, and deep acceptor levels in β-Ga_2O_3-In_2O_3 polycrystalline solid solution doped with Zr^{4+} or Ca^{2+} ions. *J. Vac. Sci. Technol. A*, *42*, 033202. https://doi.org/10.1116/6.0003466

[12] Swain, S. K., Weber, M. H., Jesenovec, J., Saleh, M., Lynn, K. G., McCloy, J. S. (2021). Compensation of Shallow Donors by Gallium Vacancies in Monoclinic β-Ga_2O_3. Phys. *Rev. Applied*, *15*, 054010. https://doi.org/10.1103/PhysRevApplied.15.054010
[13] Bhattacharjee, S., Ghosh, A. (2026). A critical perspective on temperature-dependent AC conductivity and its frequency exponent in the framework of non-overlapping small polaron tunnelling model. *Mater. Today Commun.*, *50*, 114584. https://doi.org/10.1016/j.mtcomm.2025.114584
[14] Jonscher, A. K. (1977) The 'universal' dielectric response. *Nature*, *267*, 673-679. https://doi.org/10.1038/267673a0
[15] Sidebottom, D. L., Murray-Krezan, C. M. (2002). Distinguishing Two Contributions to the Nearly Constant Loss in Ion-Conducting Glasses. *Phys. Rev. Lett.*, *89*, 195901. https://doi.org/10.1103/PhysRevLett.89.195901
[16] Natanzon, Y., Azulay, A., Amouyal, Y. (2020). Evaluation of Polaron Transport in Solids from First-principles. *Isr. J. Chem*, *60*(8-9), 768-786. https://doi.org/10.1002/ijch.201900101

СПЕКТРАЛЬНІ ТА ЕЛЕКТРИЧНІ ХАРАКТЕРИСТИКИ ЛЮМІНОФОРІВ $BaGa_2O_4$, ЛЕГОВАНИХ Mn ТА Mn-Zr

Дмитро Слободзян*, Маркіян Кушлик, В'ячеслав Васильців, Іванна Медвідь, Андрій Лучечко
Кафедра сенсорної та напівпровідникової електроніки, Львівський національний університет імені Івана Франка, вул. Ген. Тарнавського, 107, Львів, 79017, УКРАЇНА

АНОТАЦІЯ

Вступ. $BaGa_2O_4$ є широкозонним оксидом з перспективними люмінесцентними та електронними властивостями, що робить його потенційною матрицею для люмінофорних та оптоелектронних матеріалів. Контрольоване легування забезпечує ефективний підхід до модифікації його люмінесценції, дефектної структури та властивостей перенесення заряду.

Матеріали та методи. Нелегований $BaGa_2O_4$ (BGO), BGO: 0,1 мол.% Mn та BGO: 0,1 мол.% Mn, 0,2 мол.% Zr були синтезовані високотемпературним твердофазним методом. Спектри фотолюмінесценції та збудження фотолюмінесценції вимірювалися за кімнатної температури. Провідність постійного струму досліджувалася у вакуумі в діапазоні температур 370–490 K, тоді як провідність змінного струму вимірювалася в діапазоні частот 100 Гц–50 кГц з використанням амплітуди збуджувального електричного поля 5,0 В.

Результати. Нелегований BGO демонструє інтенсивну широкосмугову блакитну люмінесценцію з максимумом поблизу 410 нм, що пояснюється центрами випромінювання матриці. Легування Mn зміщує максимум випромінювання до 430–440 нм, значно зменшує інтенсивність та створює додаткову смугу збудження люмінесценції при 270–340 нм, що вказує на наявність ефективного каналу збудження, пов'язаного з центрами Mn. Спільне легування Zr додатково зменшує інтенсивність, але суттєво не змінює спектральний склад свічення. Згідно з аналізом CIE 1931, чистота кольору зменшується з 80% для BGO до 75% та 71% для зразків, легованих Mn і Mn-Zr відповідно. Електричні вимірювання показують, що легування Mn збільшує провідність постійного струму більш ніж на порядок, тоді як спільне легування Mn-Zr зменшує провідність, зберігаючи при цьому значення вище, ніж у нелегованого BGO. Енергії активації постійного струму залишаються близькими в діапазоні від 1,15 до

1,19 еВ. Провідність змінного струму демонструє частотну дисперсію, що описується універсальним законом Йоншера, причому температурна залежність показника *s* вказує на зміни в локалізованих механізмах переносу заряду.

Висновки. Легування Mn та Mn-Zr ефективно змінює оптичні та електричні властивості галату барію шляхом зміни локалізованих станів і дефектної структури. Здатність налаштовувати люмінесценцію та переносити заряд підкреслює потенціал легованого $BaGa_2O_4$ для застосування в люмінофорах та оптоелектроніці.

Ключові слова: $BaGa_2O_4$, домішки Mn-Zr, люмінесценція, електропровідність, локалізовані стани, люмінофори

Received / Одержано	Revised / Доопрацьовано	Accepted / Прийнято	Published / Опубліковано
08 July, 2026	27 August, 2026	31 August, 2026	28 September, 2026